

# A Comparative Analysis of $\text{BaTiO}_3/(\text{Ba,Sr})\text{TiO}_3$ and $\text{BaTiO}_3/(\text{Ba,Sr})\text{TiO}_3/\text{SrTiO}_3$ Artificial Superlattices via Raman Spectroscopy

Olga Aleksandrovna Maslova<sup>a\*</sup>, Yuri Ivanovich Yuzyuk<sup>b†</sup>, Nora Ortega<sup>c</sup>, Ashok Kumar<sup>d</sup>,

Ram Katiyar<sup>e</sup>, Svetlana Aleksandrovna Barannikova<sup>a,e</sup>

<sup>a</sup>Tomsk State University, Tomsk, Russia

<sup>b</sup>Southern Federal University, Rostov, Russia

<sup>c</sup>University of Puerto Rico, San Juan, Puerto Rico, USA

<sup>d</sup>CSIR-National Physical Laboratory, Dr. K. S. Krishnan Marg, New Delhi, India

<sup>e</sup>Institute of Strength Physics and Materials Science, Siberian Branch of the Russian Academy of Sciences, Tomsk, Russia

Received: June 01, 2018; Revised: August 28, 2018; Accepted: October 04, 2018

$\text{BaTiO}_3/\text{Ba}_{50}\text{Sr}_{50}\text{TiO}_3$  and  $\text{BaTiO}_3/\text{Ba}_{50}\text{Sr}_{50}\text{TiO}_3/\text{SrTiO}_3$  superlattices are characterized via Raman spectroscopy. Special attention is paid to a comprehensive analysis of their polarized Raman spectra, especially, within a soft mode ( $E(1TO)$ ) range. The shift of  $E(1TO)$  soft mode is found to be more pronounced for  $\text{BaTiO}_3/\text{Ba}_{50}\text{Sr}_{50}\text{TiO}_3/\text{SrTiO}_3$  sample than for  $\text{BaTiO}_3/\text{Ba}_{50}\text{Sr}_{50}\text{TiO}_3$ , presumably owing to stronger 2D compression of BT layers and abruptly increased temperature of transition from ferroelectric to paraelectric phase.

**Keywords:**  $\text{BaTiO}_3/\text{Ba}_{50}\text{Sr}_{50}\text{TiO}_3$ ,  $\text{BaTiO}_3/\text{Ba}_{50}\text{Sr}_{50}\text{TiO}_3/\text{SrTiO}_3$ , ferroelectric superlattices, soft mode, Raman spectroscopy, strain.

## 1. Introduction

Over the last two decades, the extensive study of structure and properties of artificial ferroelectric superlattices (SLs)<sup>1-15</sup> is due to miniaturization of electronic devices that are used in opto- and microelectronics. Strain, caused by a structural mismatch of lattices with different parameters in the plane of conjugation of epitaxial layers, favors high polarization and piezoresponse<sup>1,3,6,11,12</sup> that can exceed values typical of materials composing SLs. The unique characteristics of SLs, which are different from their bulk analogues (e.g., the great permittivity that possesses the weak dependence on temperature over a wide range, non-linear electric properties, and particular phase states) are often attributed to the combined influence of strain and electrostatic interplay of layers with different permittivity and polarization in the presence of interfaces between layers<sup>3,10,15</sup>. They can even be enhanced via the component's thickness variation in such structures, which alters the strain of layers<sup>1,7,11</sup>.

The use of SLs comprising three alternating layers with different composition expands the range of possible characteristics that can find application in electronics, many thanks to a lack of the inversion center in the symmetry elements of SLs<sup>14-16</sup>, which is not always the case of bilayer SLs. The differentiation between two types of SLs can be achieved via Raman spectroscopy that is a powerful and non-destructive tool for monitoring phase transitions and lattice dynamics<sup>17-20</sup> that impact the electric and physical properties of these structures.

The present work is aimed at studying the lattice dynamics of two-layer  $\text{BaTiO}_3/\text{Ba}_{50}\text{Sr}_{50}\text{TiO}_3$  (BT/BST) and three-layer  $\text{BaTiO}_3/\text{Ba}_{50}\text{Sr}_{50}\text{TiO}_3/\text{SrTiO}_3$  (BT/BST/ST) superlattices grown onto MgO substrates via the pulsed laser deposition. A comparative analysis of their polarized Raman spectra, particularly, within the soft-mode ( $E(1TO)$ ) range, is of particular interest to establish the structural peculiarities caused by misfits of constituting layers.

## 2. Experimental

$\text{BaTiO}_3/\text{Ba}_{50}\text{Sr}_{50}\text{TiO}_3$  (BT/BST) and  $\text{BaTiO}_3/\text{Ba}_{50}\text{Sr}_{50}\text{TiO}_3/\text{SrTiO}_3$  (BT/BST/ST) SLs were grown onto (001) single-crystal MgO substrates via the pulsed laser deposition<sup>18</sup> by the alternating focus of a laser beam on BT, BST, and ST targets (see a schematic in<sup>21</sup>). The modulation period  $\Lambda$  of BT/BST layers in a two-layer BT/BST SL was 130 Å (the thickness of individual layers was 65 Å) and that of BT/BST/ST layers in a three-layer BT/BST/ST SL enriched 150 Å (resulting in a 50-Å thickness of the constituting layers). The total thickness of heterostructures was 1 μm.

Raman spectra were excited at room temperature with an argon laser ( $\lambda = 514.5$  nm) and recorded by an Invia Reflex Renishaw spectrometer equipped with a near-excitation tunable (NExT) filter for the low-frequency spectral range analysis. The exciting radiation was focused atop a sample with a Leica optical microscope in a spot with a diameter of 2 μm. Polarized Raman spectra were collected on samples oriented with respect to crystallographic axes of substrates as  $X \parallel 100$ ,  $Y \parallel 010$ , and  $Z \parallel 001$ . Spectra with pronounced  $E$ -type

\*e-mail: o\_maslova@rambler.ru

†in memoriam

soft modes were acquired in the side-view backscattering<sup>19</sup>, at which the wave vector of the incident beam is parallel to the substrate, and the polarization of incident and scattered light is parallel or perpendicular to the  $Z$  axis of the film.

### 3. Results and Discussion

Figure 1 displays the Raman spectra of both types of SLs in cross- ( $Y(ZX)\bar{Y}$ ,  $Z(YX)\bar{Z}$ ) ( $ZX$  and  $YX$  hereinafter) and parallel- ( $Y(XX)\bar{Y}$ ,  $Y(ZZ)\bar{Y}$ ) and  $Z(YY)\bar{Z}$  ( $XX$ ,  $ZZ$  and  $YY$  hereinafter) back-scattering geometries.

One can distinguish the lines, which are typical of barium titanate-based ferroelectrics in Raman scattering, among them those denoted as  $E$  are permitted for polarizability tensor components of  $\alpha_{zx} = \alpha_{xz}$  and  $\alpha_{yz} = \alpha_{zy}$ , while those of  $A_1$  are Raman-active in the diagonal components of  $\alpha_{xx} = \alpha_{yy} = \alpha_{zz}$ , and  $B_1$  is allowed for  $\alpha_{xx}$  and  $\alpha_{yy}$  components<sup>22</sup>. The long-range electrostatic forces make all  $A_1$  and  $E$  modes splitting in transverse (TO) and longitudinal (LO) components. A band indicated as A ( $\sim 138\text{ cm}^{-1}$ ) is attributed to local distortions of the crystalline structure, which lead to the translation symmetry violation with substituting Sr for Ba in BST layers. It is interpreted as the disorder-induced phonon state density of acoustic transverse (TA) and longitudinal (LA) branches that possess the high density near the Brillouin zone boundary

<sup>23</sup>, and occurs in all back-scattering geometries of BST films<sup>17,24,25</sup>. For both SLs, one observes the depolarization of spectra in cross- and parallel-polarized configurations. Special attention is paid to the behavior of  $E(1TO)$  line which is attributed to the transverse optical vibration of soft modes  $E$  that split in various components with reducing symmetry of  $ABO_3$ -type perovskites, i.e., when perovskite enters the polar phase. This low-frequency ferroelectric mode is highly sensitive to strains emerging in perovskites, especially in thin films and superlattice which are favorable media for misfit strains due to the lattice parameter mismatch between film and substrate, or between constituting layers. The shape and spectral characteristics of  $E(1TO)$  mode (full width at half maximum, peak position) in the Raman spectrum will depend on the magnitude of strain in the probed material. As follows from the analysis,  $E(1TO)$  soft mode in  $ZX$  spectra is underdamped (with a frequency exceeding a width) for both SLs. However, in the case of BT/BST/ST SL its frequency is estimated to be  $111\text{ cm}^{-1}$  that is substantially greater than a value of  $75\text{ cm}^{-1}$  for BT/BST SL, whereas the FWHMs are  $124$  and  $111\text{ cm}^{-1}$ , respectively (see Fig. 2a). Since this mode refers to the displacement of Ti ions relative to the oxygen octahedron in the plane parallel to the substrate, its frequency is sensitive to the two-dimension compression in heterostructures. Its upshift in a three-layer SL means

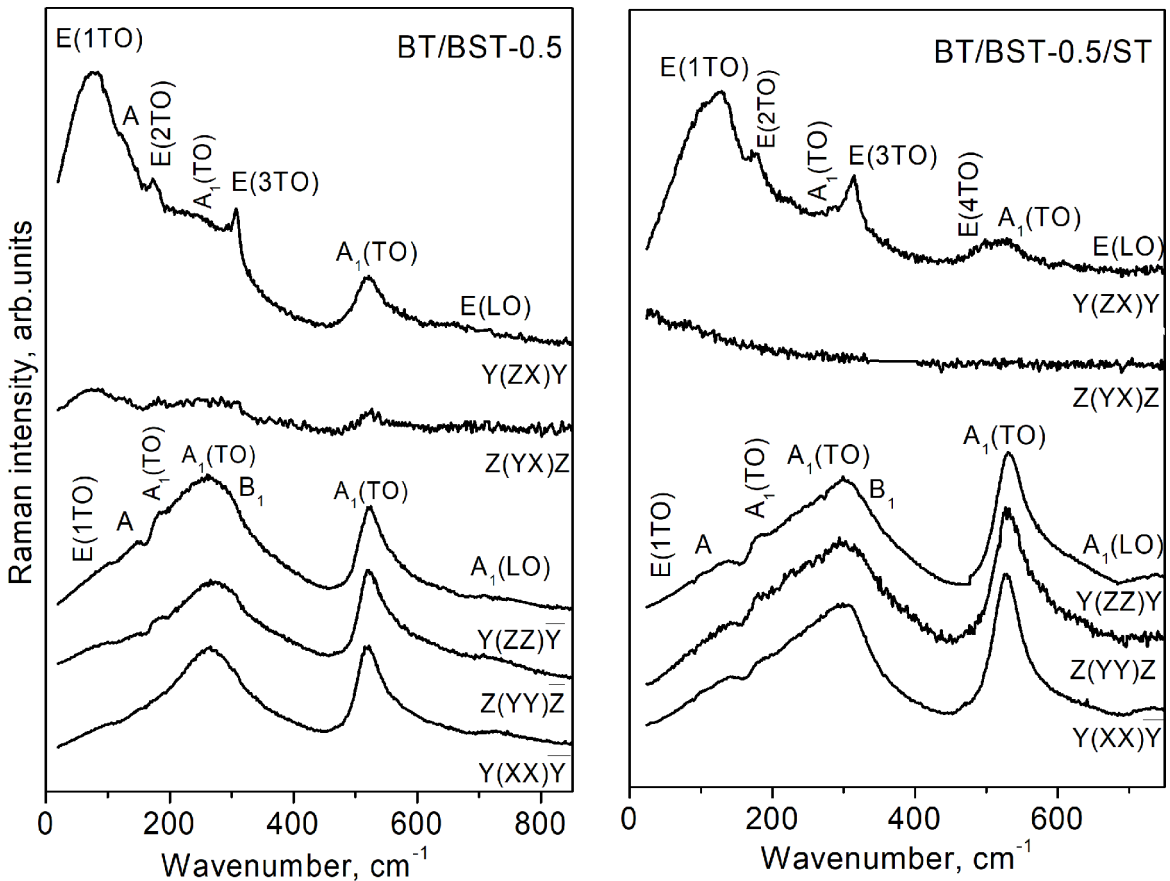


**Figure 1.** Room-temperature Raman spectra of BT/BST/ST and BT/BST SLs in different back-scattering geometries.

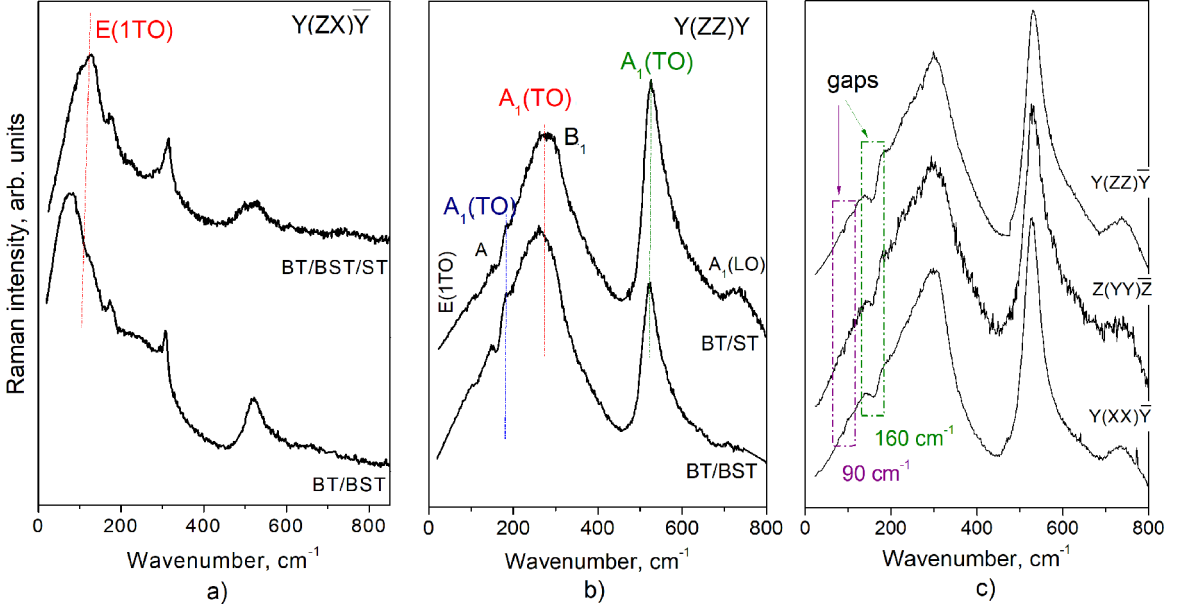


**Figure 2.** Room-temperature a) ZX and b) ZZ Raman spectra of BT/BST/ST and BT/BST SLs. The dashed lines designate the shifts of maxima of a) E(1TO) and b)  $A_1$ (TO) soft modes in Raman spectra of BT/BST/ST SL in comparison with BT/BST SL. c) Parallel-polarized Raman spectra of BT/BST/ST. The dashed contours show the interference gaps.

a drastic increase in 2D stress in the latter. As is known from the phenomenological theory<sup>26,27</sup>, this should lead to a rise in transition temperature from the ferroelectric to the paraelectric state and to the appropriate changes in electric and physical properties that are determined by the 2D compression of layers.

Another curious observation is that YX spectrum of BT/BST/ST is visually silent in comparison with a quite well-resolved YX spectrum for BT/BST SL (see Fig.1). According to the Raman selection rules<sup>22</sup>, a lack of modes in this back-scattering geometry is characteristic of *c*-domain BST films with the tetragonal symmetry of the unit cell.

The  $E$ (TO) soft mode leakage from ZX spectra also arises in diagonal back-scattering geometries (Fig. 1). Furthermore, the maxima of  $A_1$ (2TO),  $A_1$ (3TO) and  $B_1$  modes in ZZ spectrum of BT/BST/ST SL are upshifted, enriching 298, 530 and 317  $\text{cm}^{-1}$  against 261, 521 and 294  $\text{cm}^{-1}$  in ZZ spectrum of BT/BST SL, respectively (see Fig. 2b). Another important feature is the emergence of the interference gap at  $\sim 160 \text{ cm}^{-1}$  in XX spectrum of BT/BST/ST SL. Typically, this spectral peculiarity arises in ZZ configuration of the tetragonal crystal<sup>22</sup> as a result of the interaction of two  $A_1$ (TO) modes and also occurs in *c*-domain BST films<sup>24,28</sup>. However, its presence in XX geometry is unexpected for the mentioned systems. Moreover, small-depth gaps are also observed at  $\sim 90 \text{ cm}^{-1}$  in parallel-polarized spectra of BT/BST/ST SL, by analogue with those at 160  $\text{cm}^{-1}$  (see Fig. 2c), but their origin is still unclear.

Based on the results for both SLs, one can assume that, for a two-layer BT/BST SL, strain caused by the lattice parameter mismatch of the constituting layers induce the slope

of the resulting polar axis in the unit cells of SL. As earlier established, the symmetry was lowering from tetragonal of BT/ST structures to orthorhombic or even monoclinic for BT/BST SL<sup>17,18</sup>.

In BT/BST/ST SL, the upshift of E(1TO) component from 75  $\text{cm}^{-1}$  (for BT/BST SL) to 111  $\text{cm}^{-1}$  together with a “silent” YX spectrum enables the suggestion that 2D compression in this structure is much greater than in a two-layer SL. Furthermore, as established in<sup>21</sup>, the out-of-plane (*c*) parameter of BT layers in BT/BST/ST SL exceeds to a large extent that in BT/BST SL (from 4.022 to 4.080 Å). Such an amplification in tetragonality of BT layers in a three-layer SL due to the compression in the conjugation plane with ST layers results in a gain in E(TO) soft mode frequency and in a “silent” YX spectrum. In turn, BST layers should be extended because their *c* parameter ( $c_{\text{BST}} = 3.935 \text{ Å}$ ) is found to be smaller than the bulk value ( $c_{\text{BSTbulk}} = 3.947 \text{ Å}$ ), while *c* parameter of ST layers ( $c_{\text{ST}} = 3.926 \text{ Å}$ ) augments in comparison with a bulk value ( $c_{\text{STbulk}} = 3.905 \text{ Å}$ ) owing to enlarged volume of the unit cell. According to Tikhonov et al.<sup>29</sup>, such a lattice parameter distortion in a three-layer BT/BST-0.5/ST SL shifts the ferroelectric-to-paraelectric phase transition point to 610 K against 540 K for a two-layer SL.

It is worth noting that unit cell parameters of BT, BST and ST layers and, consequently, the behavior of 2D compression in SLs are also sensitive to other competitive factors, such as electrostatic and mechanical interaction between layers, or even the interplay between SL and substrate. Indeed, thermoelastic stresses induced by the substrate exert influence on the behavior of ferroelectric phase transitions emerged in barium titanate-based films. Since the soft mode in BT

corresponds to the displacement of Ti ions with respect to the oxygen octahedron, the frequency of this mode depends on the Ti-O bond length. In a tetragonal *c*-domain thin film, the E(TO) soft mode is attributed to the displacement of Ti ions in the plane parallel to the substrate, and the increase in its frequency can be due to the two-dimensional compression that arises in heteroepitaxial films because of the lattice parameter mismatch between BT and MgO. Although we do not specially consider the effect of MgO substrate on our superlattices, it has to be mentioned that the influence of substrate/film interface on the behavior of soft modes, has been clearly demonstrated in<sup>30</sup> on a heteroepitaxial (Ba,Sr)TiO<sub>3</sub> thin film grown onto a MgO substrate. For this, one edge of film was riddled from the substrate by selective chemical etching of the film. The subsequent characterization of the film at various points of its surface, including the part liberated from the substrate, revealed the substantial transformation of the E(TO) soft mode, while moving from the part bound to the substrate towards the areas beyond it. The main observation was that, being a well pronounced peak centered at 64 cm<sup>-1</sup> with a width of 57 cm<sup>-1</sup> at the beginning of the laser beam movement, the E(TO) mode becomes a wide wing with a frequency at 35 cm<sup>-1</sup> with a damping above 100 cm<sup>-1</sup> at the area of the film surface free of the substrate. The two-dimensional stress for this film was shown to drop to almost a zero value with approaching the substrate-free area. This allows the conclusion that the two-dimensional compression should vanish in the heteroepitaxial film or SL being partially or totally free of the substrate.

## 4. Conclusions

BaTiO<sub>3</sub>/Ba<sub>50</sub>Sr<sub>50</sub>TiO<sub>3</sub> and BaTiO<sub>3</sub>/Ba<sub>50</sub>Sr<sub>50</sub>TiO<sub>3</sub>/SrTiO<sub>3</sub> superlattices were thoroughly inspected via Raman spectroscopy. Special attention was paid to a comprehensive analysis of their polarized Raman spectra, especially, within a soft mode range. For a three-layer BaTiO<sub>3</sub>/Ba<sub>50</sub>Sr<sub>50</sub>TiO<sub>3</sub>/SrTiO<sub>3</sub> system, there was established a more pronounced shift of E(TO) and A<sub>1</sub>(TO) soft mode components in comparison with BaTiO<sub>3</sub>/Ba<sub>50</sub>Sr<sub>50</sub>TiO<sub>3</sub>. Spectral peculiarities, found for BaTiO<sub>3</sub>/Ba<sub>50</sub>Sr<sub>50</sub>TiO<sub>3</sub>/SrTiO<sub>3</sub> superlattice, evidenced an abrupt increase in 2D compression of BT layers, being in conjugation with ST ones, as well as more pronounced tetragonality of its unit cell against BaTiO<sub>3</sub>/Ba<sub>50</sub>Sr<sub>50</sub>TiO<sub>3</sub> structure, presumably owing to substantially risen temperature of transition from ferroelectric to paraelectric phase.

## 5. Acknowledgments

This work was partially performed within the Program of Fundamental Research of State Academies of Sciences for the period of 2013-2020 and was partially supported by Tomsk State University in the framework of the competitiveness improvement program for two authors (O.A. Maslova and

S.A. Barannikova). Experiments carried out at the University of Puerto Rico were supported by the DOD-AFOSR Grant #FA9550-16-1-0295.

## 6. References

1. Tabata H, Tanaka H, Kawai T. Formation of artificial BaTiO<sub>3</sub>/SrTiO<sub>3</sub> superlattices using pulsed laser deposition and their dielectric properties. *Applied Physics Letters*. 1994;65(15):1970.
2. Marrec FL, Farhi R, El Marssi M, Dellis JL, Karkut G, Ariosa D. Ferroelectric PbTiO<sub>3</sub>/BaTiO<sub>3</sub> superlattices: Growth anomalies and confined modes. *Physical Review B*. 2000;61(10):R6447.
3. Neaton JB, Rabe KM. Theory of polarization enhancement in epitaxial BaTiO<sub>3</sub>/SrTiO<sub>3</sub> superlattices. *Applied Physics Letters*. 2003;82(10):1586-1588.
4. Das RR, Yuzyuk YI, Bhattacharya P, Gupta V, Katiyar RS. Folded acoustic phonons and soft mode dynamics in BaTiO<sub>3</sub>/SrTiO<sub>3</sub> superlattices. *Physical Review B*. 2004;69(13):132302.
5. Diéguez O, Rabe KM, Vanderbilt D. First-principles study of epitaxial strain in perovskites. *Physical Review B*. 2005;72(14):144101.
6. Nakhmanson SM, Rabe KM, Vanderbilt D. Polarization enhancement in two- and three-component ferroelectric superlattices. *Applied Physics Letters*. 2005;87(10):102906.
7. Harigai T, Nam SM, Kakemoto H, Wada S, Saito K, Tsurumi T. Structural and dielectric properties of perovskite-type artificial superlattices. *Thin Solid Films*. 2006;509(1-2):13-17.
8. Stephanovich VA, Luk'yanchuk IA, Karkut MG. Domain-Enhanced Interlayer Coupling in Ferroelectric/Paraelectric Superlattices. *Physical Review Letters*. 2005;94(4):047601.
9. Lebedev AI. Properties of BaTiO<sub>3</sub>/BaZrO<sub>3</sub> ferroelectric superlattices with competing instabilities. *Condensed Matter arXiv*. 2013;1304:7596.
10. Bousquet E, Dawber M, Stucki N, Lichtensteiger C, Hermet P, Gariglio S, et al. Improper ferroelectricity in perovskite oxide artificial superlattices. *Nature*. 2008;452(7188):732-736.
11. Kim L, Jung D, Kim J, Kim YS, Lee J. Strain manipulation in BaTiO<sub>3</sub>/SrTiO<sub>3</sub> artificial lattice toward high dielectric constant and its nonlinearity. *Applied Physics Letters*. 2003;82(13):2118-2120.
12. Sinsheimer J, Callori SJ, Bein B, Benkara Y, Daley J, Coraor J, et al. Engineering Polarization Rotation in a Ferroelectric Superlattice. *Physical Review Letters*. 2012;109(16):167601.
13. El Marssi M, Gagou Y, Belhadi J, De Guerville F, Yuzyuk YI, Raevski IP. Ferroelectric BaTiO<sub>3</sub>/BaZrO<sub>3</sub> superlattices: X-ray diffraction, Raman spectroscopy, and polarization hysteresis loops. *Journal of Applied Physics*. 2010;108(8):084104.
14. Sai N, Meyer B, Vanderbilt D. Compositional Inversion Symmetry Breaking in Ferroelectric Perovskites. *Physical Review Letters*. 2000;84(24):5636.
15. Lee HN, Christen HM, Chisholm MF, Rouleau CM, Lowndes DH. Strong polarization enhancement in asymmetric three-component ferroelectric superlattices. *Nature*. 2005;433(7024):395-399.

16. Ogawa Y, Yamada H, Ogasawara T, Arima T, Okamoto H, Kawasaki M, et al. Nonlinear Magneto-Optical Kerr Rotation of an Oxide Superlattice with Artificially Broken Symmetry. *Physical Review Letters*. 2003;90(21):217403.
17. Maslova OA, Zakharchenko IN, Bunina OA, Yuzyuk YI, Ortega N, Kumar A, et al. A comparative study of the BaTiO<sub>3</sub> film and the BaTiO<sub>3</sub>/(Ba<sub>0.7</sub>Sr<sub>0.3</sub>)TiO<sub>3</sub> superlattice using X-ray diffraction and raman spectroscopy. *Physics of the Solid State*. 2012;54(8):1628-1634.
18. Ortega N, Kumar A, Maslova OA, Yuzyuk YI, Scott JF, Katiyar RS. Effect of periodicity and composition in artificial BaTiO<sub>3</sub>/(Ba,Sr)TiO<sub>3</sub> superlattices. *Physical Review B*. 2011;83(14):144108.
19. Yuzyuk YI, Almeida A, Chaves MR, Alyoshin VA, Zakharchenko IN, Sviridov EV. Soft Mode in Heteroepitaxial (Ba, Sr)TiO<sub>3</sub>/MgO Thin Films. *Physica Status Solidi B*. 2000;222(2):535-540.
20. Yuzyuk YI. Raman Scattering Spectra of Ceramics, Films, and Superlattices of Ferroelectric Perovskites: A Review. *Physics of the Solid State*. 2012;54(5):1026-1059.
21. Tikhonov YA, Zakharchenko IN, Maslova OA, Yuzyuk YI, Ortega N, Kumar A, et al. X-Ray diffraction and Raman spectroscopy studies of superlattices BaTiO<sub>3</sub>/(Ba<sub>0.5</sub>Sr<sub>0.5</sub>)TiO<sub>3</sub>/SrTiO<sub>3</sub>. *Physics of the Solid State*. 2014;56(3):594-598.
22. Scalabrin A, Chaves AS, Shim DS, Porto SPS. Temperature dependence of the A1 and E optical phonons in BaTiO<sub>3</sub>. *Physica Status Solidi B*. 1977;79(2):731-742.
23. Lemanov VV. Concentration dependence of phonon mode frequencies and the Grüneisen coefficients in BaxSr1-xTiO<sub>3</sub> solid solutions. *Physics of the Solid State*. 1997;39(2):318-322.
24. Yuzyuk YI, Alyoshin VA, Zakharchenko IN, Sviridov EV, Almeida A, Chaves MR. Polarization-dependent Raman spectra of heteroepitaxial (Ba,Sr)TiO<sub>3</sub>/MgO thin films. *Physical Review B*. 2002;65(13):134107.
25. Yuzyuk YI, Simon P, Zakharchenko IN, Alyoshin VA, Sviridov EV. Stress effect on the ferroelectric-to-paraelectric phase transition in heteroepitaxial (Ba,Sr)TiO<sub>3</sub>/(001)MgO thin film studied by Raman scattering and x-ray diffraction. *Physical Review B*. 2002;66(5):052103.
26. Shirokov VB, Yuzyuk YI, Dkhil B, Lemanov VV. Phenomenological theory of phase transitions in epitaxial BaTiO<sub>3</sub> thin films. *Physical Review B*. 2007;75(22):224116.
27. Shirokov VB, Yuzyuk YI, Dkhil B, Lemanov VV. Phenomenological theory of phase transitions in epitaxial BaxSr1-xTiO<sub>3</sub> thin films. *Physical Review B*. 2009;79(14):144118.
28. Lebedev AI. Dielectric, piezoelectric, and elastic properties of BaTiO<sub>3</sub>/SrTiO<sub>3</sub> ferroelectric superlattices from first principles. *Journal of Advanced Dielectrics*. 2012;2(1):1250003.
29. Tikhonov YA, Razumnaya AG, Maslova OA, Zakharchenko IN, Yuzyuk YI, Ortega N, et al. Phase transitions in two- and three-component perovskite superlattices. *Physics of the Solid State*. 2015;57(3):486-490.
30. Yuzyuk YI, Katiyar RS, Alyoshin VA, Zakharchenko IN, Markov DA, Sviridov EV. Stress relaxation in heteroepitaxial (Ba,Sr)TiO<sub>3</sub>/(001)MgO thin film studied by micro-Raman spectroscopy. *Physical Review B*. 2003;68(10):104104.